Intravenous Grafts of Human Amniotic Fluid-Derived Stem Cells Reduce Behavioral Deficits in Experimental Ischemic Stroke

Tatiana Taís Sibov[1], Lorena Favaro Pavon[1], Francisco Romero Cabral[2], Ivone Farias Cunha[2], Daniela Mara de Oliveira[3], Jean Gabriel de Souza[4], Luciana Cavalheiro Marti[2], Edgar Ferreira da Cruz[5], Jackeline Moraes Malheiros[6], Fernando F. Paiva[6], Alberto Tannús[6], Sérgio Mascarenhas de Oliveira[6], Marcos Devanir Silva da Costa[1] [iD], Patrícia A. Dastoli[1], Jardel N. Mendonça[1], Silvia Regina Caminada de Toledo[8], Suzana M. Fleury Malheiros[2,9], Manoel Antonio de Paiva Neto[1], Nelma Bastos Bezerra Rego[7], Antônio Fernandes Moron[7], and Sérgio Cavalheiro[1]

Abstract

Amniotic fluid has been investigated as new cell source for stem cells in the development of future cell-based transplantation. This study reports isolation of viable human amniotic fluid-derived stem cells, labeled with multimodal iron oxide nanoparticles, and its effect on focal cerebral ischemia–reperfusion injury in Wistar rats. Middle cerebral artery occlusion of 60 min followed by reperfusion for 1 h, 6 h, and 24 h was employed in the present study to produce ischemia and reperfusion-induced cerebral injury in rats. Tests were employed to assess the functional outcome of the sensorimotor center activity in the brain, through a set of modified neurological severity scores used to assess motor and exploratory capacity 24 h, 14, and 28 days after receiving cellular therapy via tail vein. In our animal model of stroke, transplanted cells migrated to the ischemic focus, infarct volume decreased, and motor deficits improved. Therefore, we concluded that these cells appear to have beneficial effects on the ischemic brain, possibly based on their ability to enhance endogenous repair mechanisms.

[1] Department of Neurology and Neurosurgery, Escola Paulista de Medicina—Universidade Federal de São Paulo (EPM-UNIFESP), São Paulo, Brazil
[2] Hospital Israelita Albert Einstein (HIAE), Faculdade de Ciências Médicas da Santa Casa de São Paulo, São Paulo, Brazil
[3] Department of Genetics and Morphology, Universidade de Brasilia, São Paulo, Brazil
[4] Biochemistry and Biophysics Laboratory, Butantan Institute, São Paulo, Brazil
[5] Department of Medicine, Discipline of Nephrology, Escola Paulista de Medicina—Universidade Federal de São Paulo (EPM-UNIFESP), São Paulo, Brazil
[6] São Carlos Institute of Physics, São Paulo University, São Paulo, Brazil
[7] Department of Obstetrics, Escola Paulista de Medicina—Universidade Federal de São Paulo (EPM-UNIFESP), São Paulo, Brazil
[8] Pediatrics Oncology Institute, GRAACC (Grupo de Apoio ao Adolescente e a Criança com Câncer), Escola Paulista de Medicina, Universidade Federal de São Paulo, São Paulo, Brazil
[9] Department of Neuro-Oncology, Escola Paulista de Medicina—Universidade Federal de São Paulo (EPM-UNIFESP), São Paulo, Brazil

Submitted: October 11, 2018. Revised: January 31, 2019. Accepted: May 2, 2019.

Corresponding Author:
Tatiana Taís Sibov, Universidade Federal de Sao Paulo, Rua Napoleão de Barros, 626, Sao Paulo, 04024-002, Brazil.
Email: tatisibov@gmail.com

Introduction

According to the American Heart Association, stroke is the fifth leading cause of death and the leading cause of disability in the United States[1–3]. The only FDA-approved drug for ischemic stroke is tissue plasminogen activator (tPA). Owing to the limited therapeutic window (4.5 h from disease onset to tPA administration) and the risks associated with tPA (i.e., hemorrhagic transformation), only about 3% of ischemic stroke patients actually benefit from tPA therapy[1,3–5]. With the aim of expanding the therapeutic window, novel treatment strategies target a longer delay post-stroke, specifically the restorative phase, which begins days to weeks post-stroke[3,6–9].

Stem cell therapy is an emerging therapeutic modality in the treatment of stroke. Its basis arises from the observation that certain parts of the adult brain are capable of regeneration[10–14]. Neurogenesis in the adult brain has been demonstrated in the dentate nucleus of the hippocampus and the subventricular zone. It has been shown in studies with ischemic stroke that neurogenesis happens in the ischemic penumbra, where cells were found to preferentially locate themselves in the proximity of blood vessels[14,15]. Thus, post-stroke compensatory neurogenesis may contribute to recovery after the insult. While the regenerative capacity of certain parts of the brain has been demonstrated, it is clear that this endogenous repair process is unable to overcome the wasting damage to brain tissue that occurs after acute and severe stroke[14]. Thus, targets for stem cell therapy include neuroprotective approaches aimed at protecting at-risk tissue during the acute phase of stroke, as well as neuroreparative approaches which may involve the direct replacement of damaged brain tissue or, alternatively, the promotion of the brain's endogenous repair processes[14]. Therefore, stem cells have emerged as a potential therapeutic agent for neurovascular diseases such as stroke, primarily due to their ability to release anti-inflammatory cytokines that can potentially modify the hostile environment associated with the secondary cell death of the ischemic brain[3]. The use of stem cells might be beneficial in cell therapy protocols for neurodegenerative and neurovascular diseases, but it requires an effective method to detect these infused stem cells in vivo. Cell tracking in vivo is an important methodology in the development of successful stem cell therapies. Our group previously showed the development and validation of an efficient in vitro protocol for labeling of adult stem cells with multimodal iron oxide nanoparticles conjugated to Rhodamine-B (MION-Rh), and subsequent use of these labeled cells in an in vivo model, showing that the infused labeled cells could be efficiently tracked, for example by magnetic resonance[16].

A number of different types of stem cells, obtained from different sources, have been shown to improve clinical and radiological outcomes in preclinical models of stroke. The choice of cell type for preclinical trial use should consider not only efficacy, but also the ease of obtaining the cells, issues regarding cell culture for expansion, the need for immunosuppression, and questions regarding dosage[14]. Preclinical evidence suggests the use of the amnion as a source of stem cells for the investigation of basic science concepts related to developmental cell biology, but also for therapeutic applications of stem cells in treating stroke and other neurological disorders[1]. Thus, human amniotic fluid stem cells (hAFSCs) represent a potential alternative novel source of stem cells. Initially the AFSCs were used only for prenatal diagnosis of a wide range of fetal abnormalities caused by genetic mutations, but it was noted that these same cells collected for genetic testing could be used, after diagnosis, for the isolation, culture, and differentiation in other cell lineages[17–20]. Human amniotic fluid obtained during the process of amniocentesis contains a heterogeneous cell population, originating from embryonic and extra-embryonic tissues. The properties of hAFSCs varies according to gestational age, and different approaches have been identified to isolate and characterize these types of stem cells[21,22]. Based on morphological and growth characteristics, the adherent hAFSCs can be classified into three main groups: epithelioid (E-type) cells, amniotic fluid-specific (AF-type) cells, and fibroblastic (F-type) cells. AF-type and F-type both appear at the beginning of cultivation, while E-type cells usually appear later and not in all fluid samples[21,22]. Several protocols have been used for the isolation and differentiation of hAFSCs. Although the majority of studies are based on c-Kit selected cells[23], other groups, including ours, have directly cultured unselected hAFSCs in media, allowing their proliferation. Based on reports, the specific properties concerning the stemness and differentiation ability are similar in unselected hAFSCs and c-Kit+ hAFSCs, both able to produce lineages representative of the three germ layers[22–25]. Studies have shown that hAFSCs express some important markers of pluripotency, such as OCT4, SOX2, SSEA4, SSEA3, c-MYC, and KFL4[23], and differentiation markers including BMP-4, nestin, AFP, HNF-4, and GATA 4. Most importantly, the immunomodulatory capacity and low immunogenicity of these cells make them promising candidates for allogeneic transplantation and clinical applications in regenerative medicine. Several studies have reported that hAFSCs are positive for antigens HLA-ABC (MHC class I), but only a small fraction are slightly positive for antigens HLA-DR (MHC class II)[22–25]. In addition, these cells appear resistant to rejection because they express immunosuppressive factors such as CD59 (protectin) and HLA-G[23]. In view of these considerations, hAFSCs have been classified as a novel type of broadly multipotent/pluripotent stem cell sharing characteristics of both embryonic and adult stem cells. In the present study, we analyzed the effects of intravenously transplanted hAFSCs labeled with MION-Rh in middle cerebral artery occlusion (MCAo) animals using cognitive and motor tests, magnetic resonance images, and subsequent histological analysis of the brain for determination of therapeutic benefits and mechanism of action associated with this cell therapy for stroke.

This is the first study in the literature using hAFSCs for treatment in a rat model of ischemic stroke. In our animal model of stroke caused by MCAo there was improvement following migration of transplanted cells to the ischemic focus, a decrease in infarct volume, and improvement of motor deficits. Thus, we conclude that these cells appear to have beneficial effects on the ischemic brain, possibly based on their ability to enhance endogenous repair mechanisms.

Materials and Methods

Collection of Human Amniotic Fluid Samples

This study was approved by the Ethics Committee of the Universidade Federal de São Paulo, Brazil. All participants provided informed consent. The human amniotic fluid samples (hAF) (20 mL each) were obtained from 10 pregnant women, aged 19–39 years, with fetuses undergoing repair of myelomeningocele, with gestational age up to 25 weeks. After collection the samples were kept in Dulbecco's modified Eagle's medium-low glucose (DMEM-LG; GIBCO/Invitrogen Corporation, Grand Island, NY, USA) and processed within 1 h.

Establishment of a Primary Cell Culture from hAFSC Samples

The hAF samples maintained in DMEM-LG (1:1 v/v) (Gibco-Invitrogen Corporation) were centrifuged at 400 g and supernatants discarded. Cell pellets were initially resuspended in Chang Medium (a-MEM, 15% embryonic stem cell-fetal bovine serum (Gibco-Invitrogen) with 18% Chang B and 2% Chang C (Irvine Scientific, Irvine, CA, USA), and plated onto 75 cm^2 culture bottles (Corning Incorporated, Corning, NY, USA) at a concentration of 10^7/mL and incubated at 37°C, 5% CO_2. After 48 h of culture, the medium was changed and non-adherent cells were removed, and the culture medium was changed to DMEM-LG supplemented with L-glutamine 200 mM, antibiotic-antimycotic 10,000 U/mL sodium penicillin, 10,000 ug/mL streptomycin sulfate, 25 ug/mL amphotericin B (GIBCO/Invitrogen Corporation) and 10% fetal bovine serum (FBS) (Gibco-Invitrogen Corporation), and changed every other day. When culture reached confluency (about 15 days after the primary culture), cells were treated with 0.05% Trypsin and 0.02% EDTA (Gibco-Invitrogen Corporation), then counted and replaced in 75 cm^2 culture bottles (Corning Incorporated). The experiments described in this work were performed with cells in the third cell passage.

Labeling of hAFSCs with MION-Rh

The MION (BioPAL Inc, Worcester, MA, USA) used for labeling the hAFSCs had an 8 nm magnetic core with a hydrodynamic size of 35 nm, a zeta potential of –31 mV, and an iron concentration of 2 mg/mL. These nanoparticles exhibit fluorescent properties when conjugated with Rh-B. The wavelength of excitation for Rh-B is 555 nm and the emission wavelength is 565–620 nm[16]. The hAFSCs at a standardized cell concentration (5 × 10^5) were incubated overnight (for about 18 h at 37°C, 5% CO_2) in 10 mL of culture medium with 40 µg of MION-Rh. After incubation, the culture medium solution was removed and the hAFSCs were washed twice with phosphate-buffered saline (PBS) to remove extracellular MION-Rh.

Intracellular Detection of MION-Rh in Labeled hAFSCs

Labeled hAFSCs were washed twice with PBS and fixed with 4% paraformaldehyde. Next, the Prussian blue method (Perls' acid ferrocyanide) was used to detect iron within the labeled cells. The cells were treated with 5% potassium ferrocyanide (Sigma-Aldrich, St. Louis, MO, USA), 5% hydrochloric acid (Merck, Darmstadt, Germany), and basic fuchsine (Sigma-Aldrich) for 5 min. This treatment induces reduction of ferric iron to the ferrous state with formation of a blue precipitate. The cells were then washed twice with PBS and analyzed by light microscopy. Subsequently, fluorescence analysis was done using diamidino-2-phenylindole (DAPI, Sigma-Aldrich) to label the cell nuclei and an Rh-B filter (530 nm and 550 nm) to detect the MION-Rh. Both analyses were performed using a fluorescence microscope (IX51 Olympus, Tokyo, Japan).

Immunophenotypic Profile of MION-Rh in Labeled hAFSCs

We analyzed cell surface expression with a pre-defined set of protein markers. These assays were performed using commercially available monoclonal antibodies, following the manufacturers' instructions. Briefly, the cells at third passage were harvested by a treatment with 0.25% Tryple Express (Gibco-Invitrogen, Carlsbad, CA, USA), washed with PBS (pH = 7.4) and stained with the selected monoclonal antibodies and incubated in the dark for 30 min at 4°C. Cells were then washed and fixed with 1% paraformaldehyde. The following human antibodies were used: CD14-FITC (clone: M5E2; BD Pharmingen, San Diego, CA, USA), CD29-PE (clone: MAR4; BD Pharmingen), CD31-PE (clone: WM59; BD Pharmingen), CD34-PE (clone: 581; BD Pharmingen), CD44-PE (clone: 515; BD Pharmingen), CD45-PerCPCy5 (clone: 2D1; BD Biosciences, San Jose, CA, USA), CD73-PE (clone: AD2; BD Pharmingen), CD90-APC (clone: 5E10; BD Pharmingen), CD106-FITC (clone: 51-10C9; BD Pharmingen), CD166-PE (clone: 3A6; BD Pharmingen), HLA-DR-PerCP-Cy5 (clone: L243; BD Biosciences), and CD105-PE (clone: 8E11; Chemicon, Temecula, CA, USA). Cells were analyzed using FACSARIA flow cytometry equipment (BD Biosciences) and data analyses were performed using FACSDIVA software (BD Biosciences) or Flow Jo Software (TreeStar, Ashland, OR, USA).

Pluripotency Markers

hAFSC samples were analyzed for the expression of cell membrane/intracellular protein markers related to pluripotency. These assays were also performed using commercially available monoclonal antibodies, following the manufacturers' instructions. Briefly, the cells at second passage were harvested by a treatment with 0.25% Tryple Express (Gibco-Invitrogen), washed with PBS (pH = 7.4) and stained with the selected monoclonal antibodies and incubated in the dark for 30 min at 4°C. Cells were then washed and fixed with 1% paraformaldehyde. The following human antibodies were used: Tra-1-60-BV450 (clone: Tra-1-60; BD Horizon, San Diego, CA, USA), CXCR4-PE-Cy7 (clone: 12G5; BD Pharmingen), CCR2-Alexia Fluor-647 (clone: 48607; BD Pharmingen), CD123- (clone: 123; BD Pharmingen), SSEA-4-PE (clone: MC813-70; BD Horizon), Sox2-PerCP (clone: Sox2; BD Pharmingen), CD44-APC-Cy7(clone: IM7; BD Pharmingen), Nanog-FITC-GFAP (clone: Nanog; BD Pharmingen), and Oct3/4- (clone: Oct3/4; BD Pharmingen). Data analyses were performed using FACSDIVA software (BD Biosciences) or Flow Jo Software (TreeStar).

G-banding Karyotype Analysis

To analyze the karyotype of MION-Rh-labeled hAFSCs, cell division was blocked in mitotic metaphase by 0.1 µg/mL colcemid (Sigma-Aldrich) for 2 h. Then the cells were trypsinized (0.05% Trypsin and 0.02% EDTA; Gibco/Invitrogen Corporation), resuspended in 0.075 M KCl solution (Merck), and incubated for 30 min at 37°C. The cells were fixed with methanol (Merck) and acetic acid (Merck) mixed in a 3:1 ratio. This procedure was repeated twice. After the last wash, the supernatant was removed, the cells resuspended and dropped on glass slides (Knittel, Microscope Slides & Cover Slips for Microscopy). After 3 days, the cells were fixed on the glass slides. The slides were placed in PBS (Merck) at 60°C and washed in water. Then the slides were covered with Wright stain (Merck) 25% and washed in water. G-band standard staining was used to observe the chromosome. Karyotypes were analyzed and reported according to the International System for Human Cytogenetic Nomenclature.

Differentiation Capacity of MION-Rh Labeled hAFSCs

To evaluate the differentiation ability of MION-Rh-labeled hAFSCs, the cells were subjected to adipogenic and osteogenic differentiation in vitro according to the method described by Sibov and colleagues[16]. Labeled cells were plated at a density of 10^4 cells/cm^2 in a six-well culture plate. Eighty percent confluence was achieved in the induction medium (DMEM-LG), which was changed every other day until 21 days, for both differentiation assays. The adipogenic culture medium contained insulin 10 µg/mL (Sigma-Aldrich), indomethacin 100 µM (Sigma-Aldrich), dexamethasone 1 µM (Sigma-Aldrich), and 3-isobutyl-1-methyl-xanthine 100 µg/mL (Sigma-Aldrich) in minimum essential medium alpha medium powder (Gibco-Invitrogen) with 10% FBS. The labeled cells were fixed with 4% paraformaldehyde and stained with 0.3% Oil-red-O (Sigma-Aldrich), according to the method described by Sibov and colleagues[16]. The osteogenic culture medium contained 1 µM dexamethasone (Sigma-Aldrich), 2 µg/mL ascorbic acid (Sigma-Aldrich), and 10 mM beta-glycerophosphate (Sigma-Aldrich). Thereafter, the cells were fixed with paraformaldehyde 4% and stained with Alizarin Red (Sigma-Aldrich), according to the method previously reported by Sibov and colleagues[16]. The morphology of the cells was imaged using an inverted microscope.

Animal Ethics Statement

All animal experiments were conducted in accordance with the guidelines for animal experimentation determined by the UNIFESP Care Committee, and approved by the Committee on the Ethics of Animal Experiments of UNIFESP. In addition, ethical conditions were maintained, assuming all international rules of animal care outlined by the International Animal Welfare Recommendations and in accordance with local institutional animal welfare guidelines. Rats were housed two per cage in a temperature- and humidity-controlled room that was maintained on 12/12 h light/dark cycles. They had free access to food and water.

Focal Ischemia Model

Eight-week-old male Wistar rats ($n = 43$) were used in the test; $n = 30$ rats receiving 2×10^6 MION-Rh-labeled hAFSCs via the caudal vein, at different times after the event. There were five groups, including unoperated healthy rats (healthy control, $n = 5$); stroke control rats, did not receive cell therapy (stroke control, $n = 8$); ischemic rats given MION-Rh-labeled hAFSCs 1 h after reperfusion ($n = 10$); ischemic rats given MION-Rh labeled hAFSCs 6 h after reperfusion ($n = 10$); and ischemic rats given MION-Rh-labeled hAFSCs 24 h after reperfusion ($n = 10$). The experimental model used is described by Koizumi et al.[26] and was modified by Longa and colleagues[27]. This ischemia model affects brain damage in regions of the cortex, hippocampus, striatum, and basal ganglia. The animals were anesthetized by halothane 1% in 3:7 (vol/vol) O_2/N_2O via face mask. Body temperature was maintained at 37°C ± 0.3°C during the surgical procedures. The midline skin incision was made in the neck with subsequent exploration of the right common carotid artery (CCA), the external carotid artery, and internal carotid artery. A 4-0 monofilament nylon suture (27.0–28.0 mm) was advanced from the CCA bifurcation until it blocked the origin of the middle cerebral artery. Animals were allowed to recover from anesthesia during MCAo. After 60 min of transient MCAo, animals were reanesthetized with halothane 1% in 3:7 (vol/vol) O_2/N_2O via face
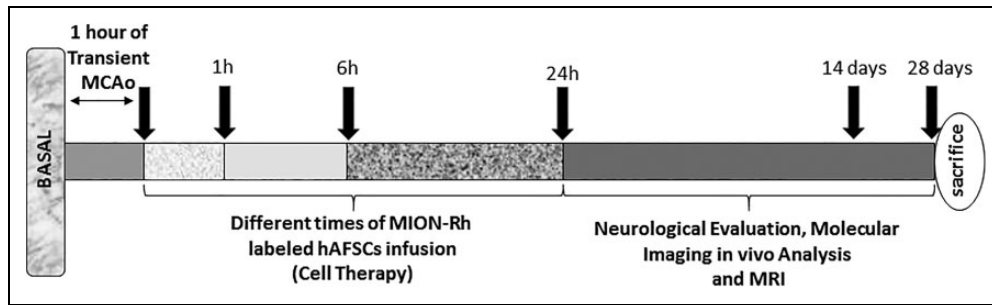
Fig. 1. Experimental design. Rats were subjected to a 1 h transient MCAo and after, at different times (1 h, 6 h, and 24h), received intravenous transplants of MION-Rh-labeled hAFSCs. After behavioral evaluations (neurological evaluations), molecular imaging in vivo analysis and magnetic resonance imaging (MRI), all rats were sacrificed for immuno- and histochemical evaluations.

mask and reperfused by withdrawal of the nylon thread. After 1 h of reperfusion the animals received MION-Rh-labeled hAFSCs, by tail vein, at different times. One animal died immediately after reperfusion, and three animals died after receiving the cell therapy; thus a mortality rate of approximately 13% was observed post-MCAo in this study. The total number of animals in each group was as follows: $n = 8$ for the MION-Rh-labeled hAFSC-infused stroke animals, after 1 h of reperfusion, $n = 9$ for the MION-Rh-labeled hAFSC-infused stroke animals, after 6 h of reperfusion, $n = 9$ for the MION-Rh-labeled hAFSCs-infused stroke animals, after 24 h of reperfusion, and control animal group. A schematic diagram of experimental design is shown in Fig. 1. Magnetic resonance imaging (MRI) and molecular imaging was used to evaluate the animals of all the groups mentioned above. After this, all animals were euthanized on day 28 post-MCAo, both treated and control animals, for subsequent immunohistochemical investigations ($n = 32$), and all animals from each group were submitted to staining and measurement of infarct volume by triphenyltetrazolium chloride-2,3,5 (Sigma-Aldrich).

Molecular Imaging in vivo

After MION-Rh-labeled hAFSCs were infused in stroke animals, these cells were monitored using an in vivo imaging device, Bruker model MS FX PRO (Bruker, Ettlingen, Germany). Throughout image acquisition, animals were placed in dorsal recumbence and remained anesthetized with inhaled 2% isoflurane in oxygen at 2 L/min. Initially, the skull images were acquired by X-ray. The fluorescence of the labeled cells was evaluated using the excitation (540 nm) and emission (585 nm) of MION-Rh. The images were acquired and evaluated using multiplex location software.

Magnetic Resonance Imaging

MRI brain scans were obtained in a 2 Tesla/30 cm horizontal superconducting magnet 85310HR (Oxford Instruments,

Abingdon, UK) interfaced to a Bruker Avance AVIII console (Bruker-Biospin) with Paravision 5.1 software (Bruker). A Crossed Saddle radiofrequency coil was used as a head probe in animals anesthetized with ketamine/xylazine (95/12 mg/kg, i.p.). A T_2-weighted RARE (Rapid Acquisition with Refocused Echoes) sequence (TR = 5000 ms, TE = 51 ms, RARE factor = 8, 24 averages, 24 min/animal) was used in a volume of $15 \times 33 \times 26$ mm^3 covered with a 96×96 matrix and 1 mm slice thickness without gaps (26 slices), generating a spatial resolution of 156×344 μm^2.

Behavioral Testing

Tests were applied to evaluate the response to stimuli in animals that received cellular therapy, at different treatment times (1, 6, and 24 h after reperfusion), after 24 h, 14, and 28 days. The first test applied was proprioception, also called kinesthesia, and evaluates the ability to recognize the spatial location of the body, its position and orientation, the force exerted by the muscles, and the position of each part of the body in relation to the others; that is, evaluates the march intensification (fore and hind limbs). Another applied test was the rat vibrissae touch, in which the stretch of the fore-limbs is observed after a stimulus has been applied in the animal's vibrissae as an examiner holds his trunk[28,29]. These evaluations were performed 10 times for each animal, with scores of 0 for normal march/stretch, and 1, 2, and 3 for march/stretch performed with different levels of difficulty subsequent to increasing values of scores and in relation to animal with movements considered within the normal range. open field tests were also performed to evaluate the exploratory capacity of these animals during a period of 10 min, in which the observed behavioral parameters were the *number of line crossings* (with all four paws) performed in an acrylic box with checkered background of 60 cm in height by 60 cm in width (assessment of locomotor activity); *number of rearing* to assess the number of times these animals were sustained only with the hind legs; and the *number of grooming* to evaluate how often the animal cleans itself using its front paws.

Histochemistry Analysis and Measurement of Infarct Volumes

After image acquisition, under deep anesthesia, rats were euthanized on day 28 post-MCAo, both treated and control animals, for immunohistochemical investigations ($n = 32$), and all animals from each group were submitted to staining and measurement of infarct volume by triphenyltetrazolium chloride-2,3,5 ($n = 4$). Briefly, animals were transcardially perfused with a buffered saline solution and 4% paraformaldehyde. The brains were removed and stored in paraformaldehyde for 24 h and cryoprotected in a 40% sucrose solution for 48 h. Coronal sections were cut to 40 μm thickness using a cryostat (Leica CM3050 S, Leica Biosystems) and stained using standard procedures for hematoxylin-eosin, periodic acid–Schiff (PAS), and Masson Trichrome staining and the proliferation marker Ki67. Coronal sections also were cut to 1 mm thickness using a cryostat (Leica) and stained using triphenyltetrazolium chloride-2,3,5 (TTC) (Sigma-Aldrich) at 37°C for 30 min to determine the viability of brain tissue. The infarcted areas were pale, while the normal brain tissue was stained red. The slices were photographed and analyzed in the image J software (NIH Image Software, Bethesda, MD, USA) to determine the infarct volume. The extent of tissue damage was calculated as a percentage of the infarct volume[30].

Statistical Analysis

All results are presented as the mean $\pm$ standard deviation (SD). Significant differences between the two mean values were compared using Student's *t*-test. One-way ANOVA with Scheffe's post hoc test was used to assess significant differences if more than two groups were compared. The results were considered statistically significant when $p < 0.05$.

Results

Establishment of a hAFSC Primary Culture and Morphological Analysis

Primary cell cultures were successfully obtained from all hAF collected samples ($n = 10$). After 1 week with medium being changed every other day, hAFSC primary cultures initially showed heterogeneous cell populations with three main groups: epithelioid cells (ECs) (Fig. 2A.b and A.d), amniotic fluid-specific cells (AFCs) (Fig. 2A.a), and fibroblastic cells (FCs) (Fig. 2A.c). AFCs and FCs both appear at the beginning of cultivation, while ECs may appear later and not in all hAF samples. After three passages of culture, hAFSCs primary culture showed a homogeneous cell population, with fibroblast-like cell morphology (Fig. 2A.g and A.h).

Detection of MION-Rh-Labeled hAFSCs Using a Fluorescence Assay

hAFCs were labeled with MION-Rh, a multimodal iron oxide nanoparticle (with fluorescent and magnetic properties) which can be visualized by both MRI and fluorescence imaging. Thus, the intracellular distribution of MION-Rh in hAFSCs was qualitatively evaluated using fluorescence microscopy with an Rh-B filter (530 nm and 550 nm). We observed that MION-Rh nanoparticles were internalized by hAFSCs and formed intracellular granules or small fluorescent red clusters (Fig. 2A.g, A.h, A.i and A.j).

Qualitative Analysis of MION-Rh-Labeled hAFSCs

A qualitative evaluation of the intracellular distribution of MION-Rh in hAFSCs was performed by cytochemical assessment using Prussian Blue and light microscopy using fuchsine. We observed the internalized MION-Rh as blue granules with intracellular localization (Fig. 2B.b, B.c), whereas the unlabeled cells (control) did not show the presence of intracellular blue granules (Fig. 2B.a). The intracellular distribution of MION-Rh in hAFSCs was also observed by fluorescence assay, and small fluorescent red clusters colocalized with the blue granules were observed on cytochemical assessment (Fig. 2B.e, B.f).

Differentiation of MION-Rh-Labeled hAFSCs

We assessed the differentiation potential of MION-Rh-labeled hAFSCs using culture medium containing adipogenic and osteogenic lineage-specific induction factors. The differentiation capacity of these cells was confirmed after 21 days in culture and was demonstrated by the Oil Red and Alizarin Red cytochemical assays (Fig. 2B). Labeled cells differentiated in adipocyte-like cells and showed the presence of lipid droplets as observed by the Oil Red staining (Fig. 2B.a), while non-differentiated labeled cells (negative control) did not show the presence of lipid droplets (Fig. 2B.b). Labeled cells also differentiated into osteoblast-like cells showing calcium deposition on the extracellular matrix as observed by the Alizarin Red assay (Fig. 2B.e), while undifferentiated labeled cells (negative control) did not show the presence of calcium (Fig. 2B.f). Unlabeled cells also showed the presence of lipid droplets (Fig. 2B.c) and calcium on the extracellular matrix (Fig. 2B.g), and its respective undifferentiated control (Fig. 2B.d and B.h).

Immunophenotypic Characterization and Pluripotency Marker Expression of MION-Rh-Labeled hAFSCs

We obtained attached hAFSC populations from all 10 collected and processed hAF samples. These cell populations were analyzed by FACS according to granularity, size, and cell surface markers. These gated cells, from culture-expanded cells (Passage 3), were analyzed for the expression of cell membrane and intracellular protein markers. FACS analysis showed the cells were strongly positive for the typical mesenchymal markers, such as CD29, CD44 (hyaluronic receptor), CD73, CD90, CD105 (endoglin), CD166, low or no expression of MHC class I antigens, HLA-DR and
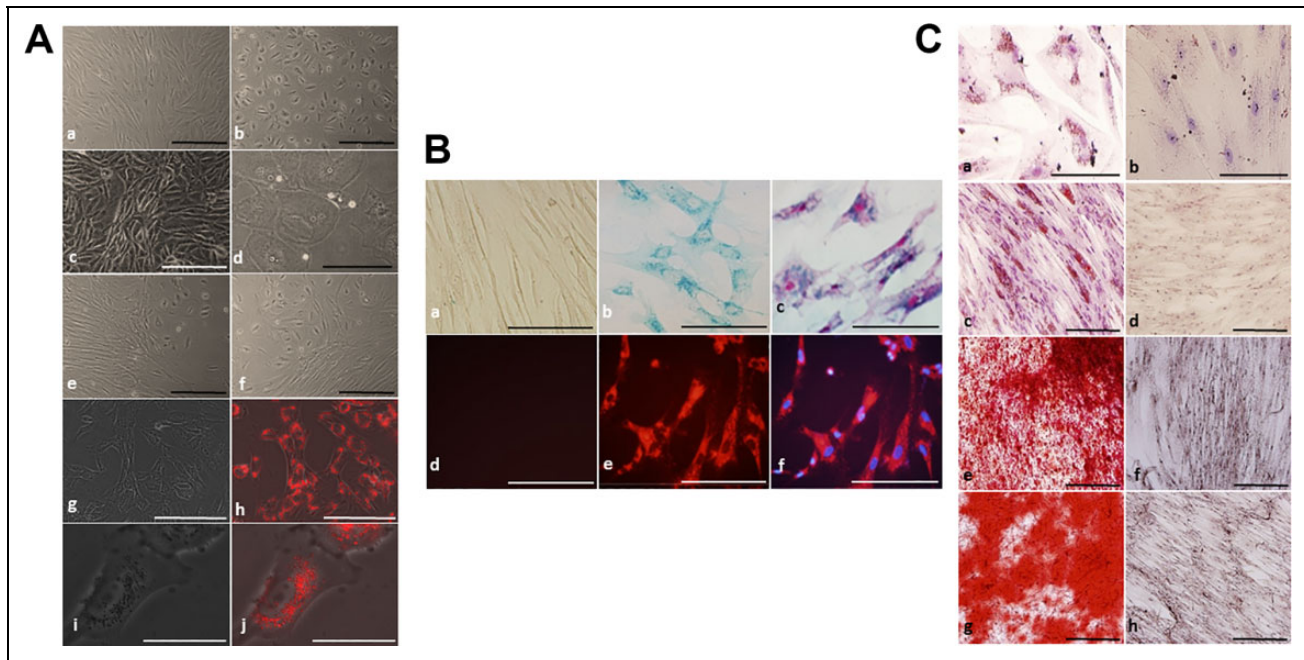
Fig. 2. (A) hAFSCs culture; a. amniotic fluid specific cells (AFCs), 100×; b, d. Epithelioid cells (ECs), 100× and 400×, respectively; c. Fibroblast cells (FCs), 100×; e, f. Heterogeneous cell population, 100×; g, h, I, and j. hAFSCs labeling with MION-Rh, 100× and 400×, respectively. (A.a, A.b, A.c, A.e, A.f, A.g and A.h) Scale bars, 200 μm; (B.a, B.b, B.e, B.f, B.g and B.h) Scale bars, 400 μm; (A.d, A.i, A.j, B.c and B.d) Scale bars, 800 μm. (B) MION-Rh-labeled hAFSCs culture; a, d. Non-labeled cells (negative control: Prussian blue and Fluorescence microscopy, scale bars 400 μm; b. Prussian blue of hAFSCs labeling with MION-Rh, 400×; e. Fluorescence microscopy of hAFSCs labeling with MION-Rh, 400×, scale bars, 800 μm, respectively. c. Prussian Blue and basic fuchsin of hAFSCs labeling with MION-Rh, 400×; f. Fluorescence microscopy (DAPI) of cell nucleus, 400×, scale bars, 800 μm, respectively. (C) Differentiation process of MION-Rh-labeled hAFSCs and non-labeled hAFSCs; a. Non-labeled cells differentiated in adipocyte-like cells, 400×; b. Non-differentiated labeled cells (negative control), 200×; c. Labeled hAFSCs differentiated into adipocyte-like cells, 200×; d. Non-differentiated labeled cells (negative control), 400×, Oil Red stained; e. Non-labeled cells differentiated into osteoblast-like cells, 200×; f. Non-differentiated non-labeled cells (negative control), 200×; g. Labeled hAFSCs differentiated in osteoblast-like cells, 200×; and h. Non-differentiated labeled into osteoblast-like cells (negative control), 200×; Alizarin Red.

hematopoietic cells markers (CD14, CD31, CD34, CD45, and CD106) and absence of MHC class II antigens (Fig. 3B). The hAFSC populations expressed the homing markers CXCR4 and CCR2 (Fig. 3B). The expression of embryonic stem cell pluripotency markers Tra-1-60, Stage Specific Embryonic Antigen 4 (SSEA-4), Sox2, Nanog, Octamer Binding Transcription factor 3/4 (Oct3/4), and CD123 was also observed in these cell populations (Fig. 3B).

Karyotype of MION-Rh Labeled hAFSCs

Karyotypes of MION-Rh-labeled hAFSCs were analyzed and reported according to the International System for Human Cytogenetic Nomenclature. Cytogenetic interpretation showed the karyotype featured in 22 pairs of autosome chromosomes and one pair of sexual chromosomes. Among the samples analyzed, karyotypes showed normal female (Fig. 3C.a) and male (Fig. 3C.b) chromosome types (46 XX and 46 XY, respectively) with no chromosome abnormalities observed.

MION-Rh-Labeled hAFSC Transplantation Decreases Infarct Volume Caused by MCAo

MRI images and TTC staining after 28 days revealed that the MION-Rh-labeled hAFSCs that were transplanted after 6 h of reperfusion in stroke animals exhibited a more significant decrease in infarcted area volume compared with the other cell therapy times analyzed (1 and 24 h). For this reason, Fig. 4 shows only the images corresponding to cell therapy after 6 h of reperfusion (Fig. 4E and 4F, respectively: representative figure of the whole group) compared with the control stroke animals (Fig. 4C and 4D, respectively: representative figure of the whole group) and with the unoperated control animal (Fig. 4A and 4B, respectively: representative figure of the whole group). There was approximately a 45% difference between the infarct volumes of the MION-Rh-labeled hAFSC-transplanted stroke animals and the control stroke animals, which equated to about a 75% reduction in infarct volume in the MION-Rh-labeled hAFSC-transplanted stroke animals ($p<0.05$) (Fig. 4G). In these animals monitored by MRI, the T2-weighted MRI showed an
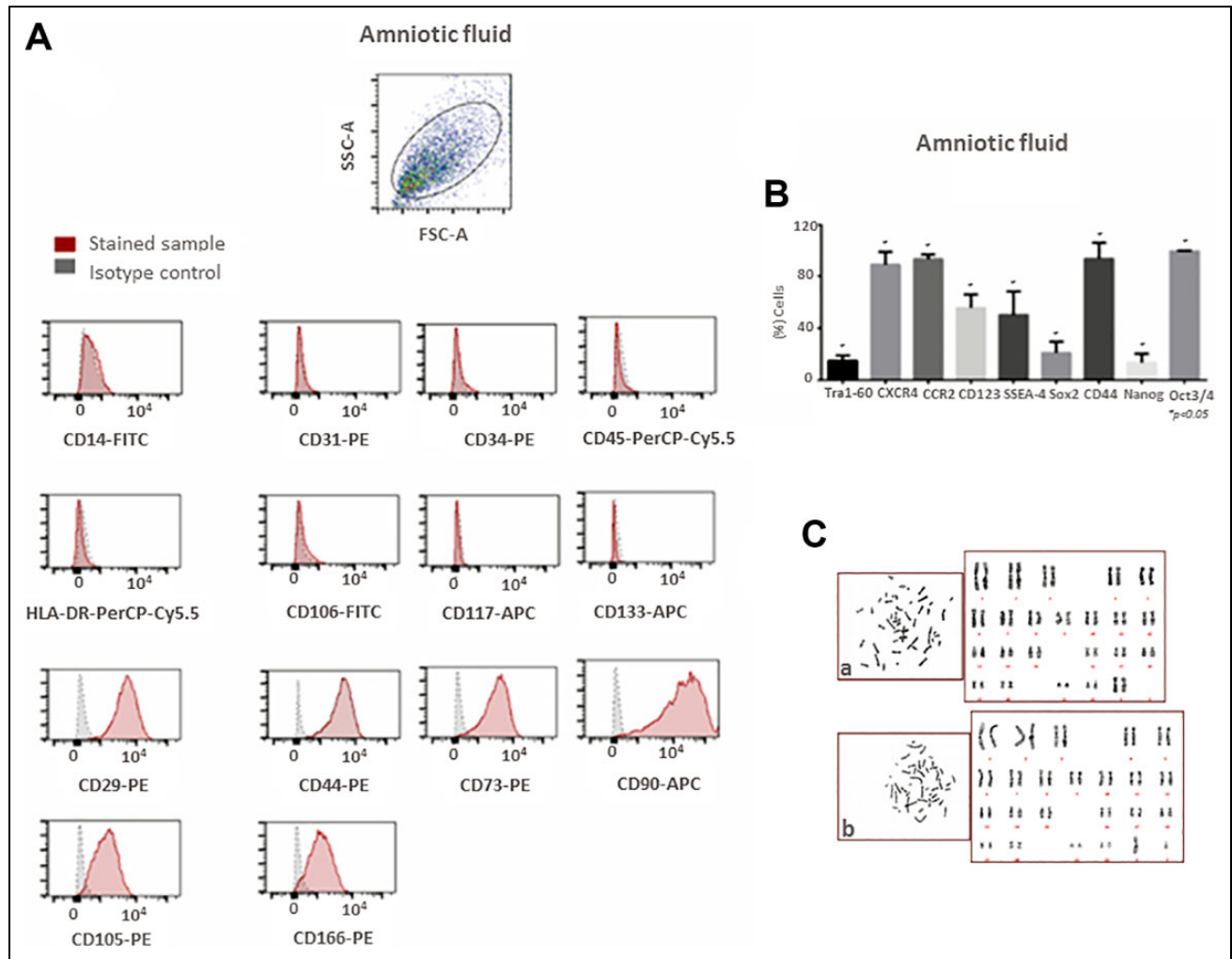
Fig. 3. Immunophenotypic characterization, pluripotency marker expression and karyotype of MION-Rh-labeled hAFSCs. (A) Immunophenotypic analyses showed that the cells expressed CD29, CD44, CD73, CD90, CD105, and CD166, did not express and/or had low levels of CD14, CD31, CD34, CD45, CD106, CD117, CD133, and HLA-DR. (B) Pluripotency markers expressed in MION-Rh-labeled hAFSCs. (C) Karyotype featured in 22 pairs of autosomal chromosomes and one pair of sexual chromosomes; a. Normal female chromosome (46, XX); b. Normal male chromosome (46XY).

attenuated infarct volume in MION-Rh-labeled hAFSC-transplanted animals, reperfused after 6 h (Fig. 5C: arrow head; representative image of the whole group) compared with the control stroke animals (Fig. 5B: arrow; representative image of the whole group). The hypersignal caused by water content of the ischemic hemisphere demonstrated in the MRI was lower in the treated stroke animals compared with control stroke animals. Unoperated control animals did not show MRI hypersignal (Fig. 5A: representative image of the whole group). The percentage of the infarct volume (edema) was 30.7% for the control stroke animal and 12.8% for the treated stroke animal.

## In vivo Tracking of MION-Rh-Labeled hAFSCs

The animals received MION-Rh-labeled hAFSC therapy by tail vein 1 h (figure not shown), 6 h (Fig. 5E: representative

figure of the whole group) and 24 h (figure not shown) after MCAo. After about 30 min, these cells crossed the blood–brain barrier and reached the penumbra area of ischemia (inflammatory area), showing homing of these cells to the injured area (Fig. 5E.b), also showed in ex vivo brain imaging (Fig. 5E.b1).

MION-Rh-Labeled hAFSC Transplantation Improves Motor Deficits Caused by MCAo

We use the rating scale for neurological disorders described by Garcia and co-workers (1995) to assess functional neurological recovery 24 h, 14, and 28 days after the different cell therapy treatment times (1, 6 and 24 h after reperfusion) (Fig. 6)[31]. The results showed that animals subjected to ischemia showed extensive ischemic infarct area (cortex, hippocampus, striatum, and basal ganglia) (Fig. 4C and 4D) and neurological deficit 24 h after ischemia, showing
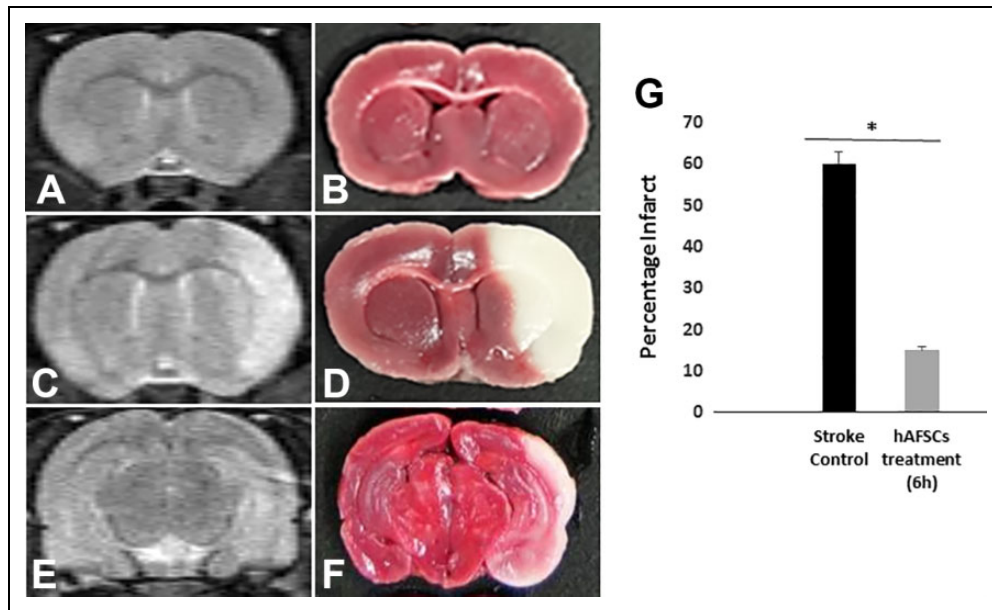
Fig. 4. Infarct volume was reduced by MION-Rh-labeled hAFSCs transplantation: representative figure. (A, C and E) Rats monitored by MRI, the T2-weighted, after 28 days; (A) control animal, (C) stroke control animal, (E) treated stroke animal (6 h); (B, D and F) TTC staining, after 28 days; (B) control animal, (D) stroke control animal, (F) treated stroke animal (6 h). (G) Data are shown as percentages of the infarct volumes present in the ipsilateral hemisphere relative to the contralateral hemisphere. Quantitative analyses revealed that percentages of the infarct volumes of rats receiving MION-Rh-labeled hAFSCs transplants are significantly reduced (*$p<0.05$).
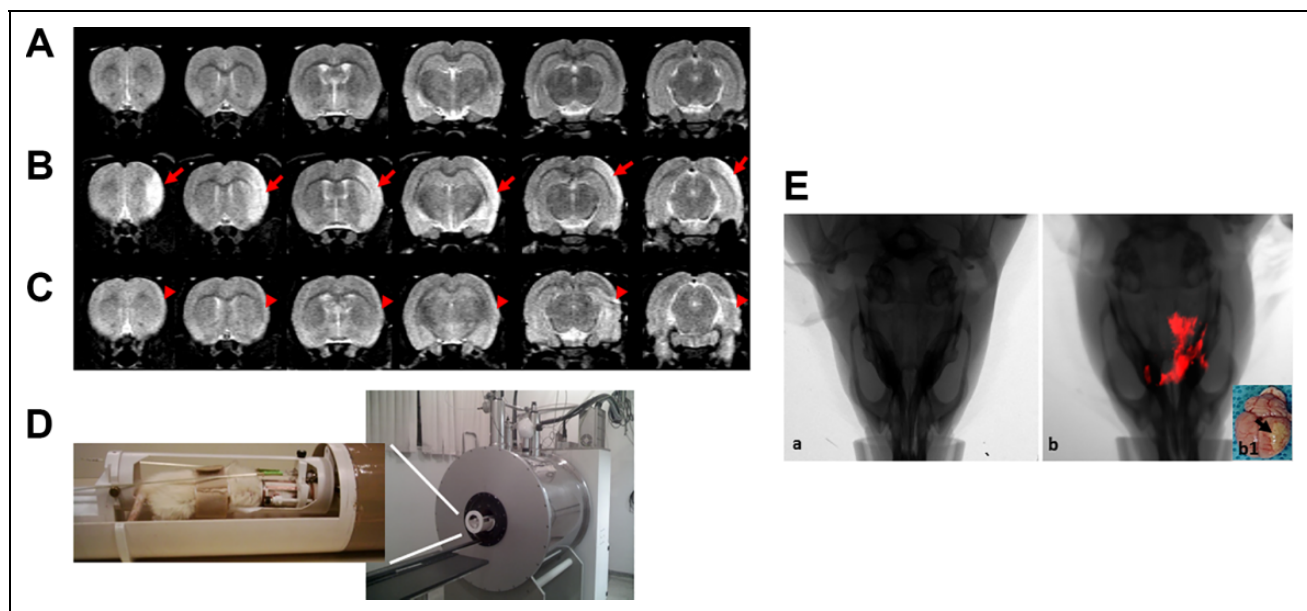
Fig. 5. MRI monitoring of in vivo MCAo; T2-weighted rapid acquisition with refocused echoes (RARE) sequence (TR = 5000 ms, TE = 51 ms, RARE factor = 8, 24 averages, 24 min/animal). (A) control animal; (B) stroke control animal; (C) treated stroke animal (6 h); (D) MRI equipment for small rodent neuroimaging: 2 Tesla superconducting magnet 85310HR; (E) Combined fluorescence and X-ray tomography for in vivo detection of MION-Rh-labeled hAFSCs, (E.a) stroke control animal (without treatment), (E.b) In vivo detection of the MION-Rh-labeled hAFSCs in "treated stroke animal (6 h)", (E.b1) Ex vivo brain imaging: arrow = region of ischemia.

a direct correlation between the size of the infarct area and neurological deficit, corroborating the results of other authors who obtained similar results. Stroke control rats consistently showed impaired motor performance when compared with healthy controls as assessed by the exploratory motor and sensory tests.
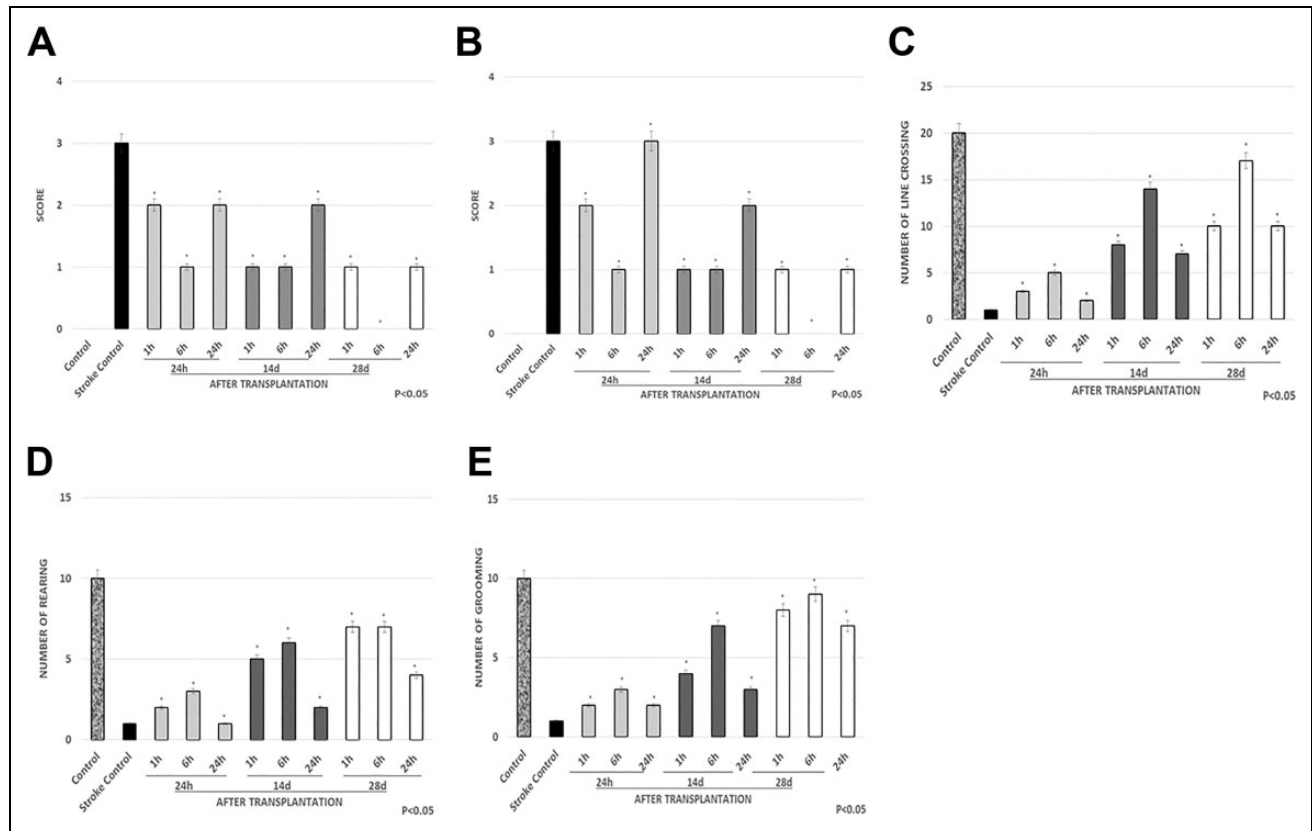
Fig. 6. Functional neurological evaluation (behavioral tests). (A) Proprioceptive test (evaluates rat gait intensification—anterior and posterior limbs); (B) Vibrissae touch test (evaluates stretching of the anterior limbs after stimulation); (C) number of line crossing (evaluates locomotor activity); (D) Number of rearing (evaluates support with hind paws); (E) Number of grooming (evaluates the use of front paws for self-cleaning). For all the tests it was observed that the 6 h group showed the best score after 14 and 28 days following transplantation. There was a significant improvement in neurological deficit (*p<0.05).

In the proprioceptive and vibrissae touch tests, at all times observed after treatment, the 6 h group ($n = 9$) showed the best score in relation to the stroke controls and other treatment groups (1 h, $n = 8$, and 24 h, n = 9), especially after 14 and 28 days, which suggests that the 6 h treatment time improved the motor deficits (Fig. 6A and 6B). A significant and similar improvement in neurological deficit, in the same treatment group (6 h), was observed in other tests after 14 days of treatment (Fig. 6C, 6D, and 6E). We observed that the number of line crossing, of rearing, and of grooming in the rat group that received MION-Rh-labeled hAFSCs after 6 h of reperfusion showed significant improvement up to 28 days after treatment when compared with healthy control animals (Fig. 6C, 6D, and 6E). Although other groups that received cells at different times post-reperfusion also showed significant improvement compared with healthy controls, they produced less significant results in relation to the aforementioned animal group.

Histochemical Analysis

Only in the histochemical image of the 6 h treated group ($n = 9$) can we identify the presence of infused MION-Rh-labeled hAFSCs, thus suggesting improvement of the penumbra area, correlating the results obtained in functional neurological recovery tests in this group of animals. In other treated groups it was not possible to correlate these results. Histological analysis (Fig. 7) demonstrated that the animals euthanized on day 28 post-MCAo, control animals without treatment, exhibited an important stroke area or ischemic core in the cortex region (Fig. 7A, 7G, and 7M). However, animals treated with MION-Rh-labeled hAFSCs (after 6 h of reperfusion), showed an increase in cell numbers in the penumbra area detected by histological analysis for PAS (Fig. 7C, 7I, and 7O), Masson's trichrome staining (Fig. 7E, 7K and 7Q); immunohistochemical assay for ki67 (cycling cell) (Fig. 7D, 7J, and 7P) and fluorescence microscopy (Fig. 7F, 7L, and 7R). We know that cells that were positive for the immunohistochemical labeling of the cell proliferation marker (Ki67) (Fig. 7D, 7J, 7P) are the hAFSCs, since they are the same cells that when observed by fluorescence were shown as marked by MION-Rh (Fig. 7F, 7L, 7R). In addition, we highlight the presence of hAFSCs in corresponding tissue areas, for example Fig. 7E,F; 7K,L; 7Q,R; this does not occur in the control (ischemic brain tissue that did not receive hAFSCs—Fig.
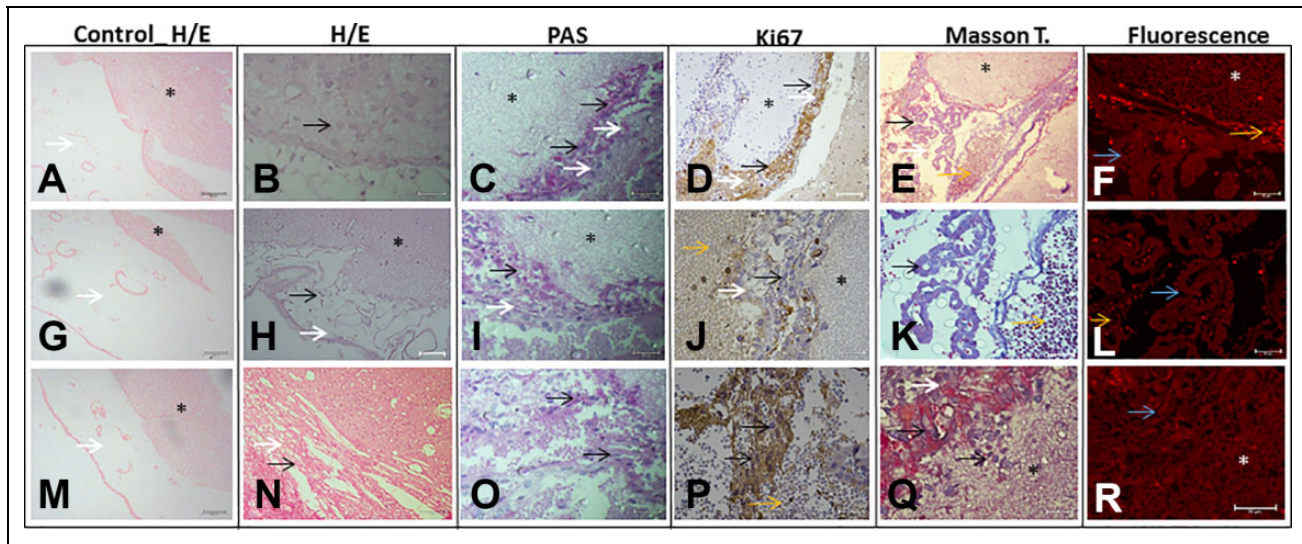
Fig. 7. Histological analysis of animal model 28 days post-MCAo. (A, G, M) Area stroke or ischemic core (*) no treatment. (B–F, H–L, N–R) Ischemic core with treatment of hAFSCs. (A, B, G, H, M, N) Hematoxylin and eosin staining; (C, I, O) Histochemical assay of periodic acid–Schiff (PAS); (D, J, P) Immunohistochemical assay of ischemic core (*) for Ki67 for detection of proliferation of hAFSCs; (E, K, Q) Masson's trichrome staining; (F, L, R) Fluorescence microscopy. Area penumbra (white arrow). hAFSCs can be observed in the area penumbra (black and blue arrow). Blood cells (yellow arrow). Scale: 50 μm.

7A, 7G, 7M) compared with the penumbra area of the ischemic core, where the hAFSCs are clearly present (Fig. 7C, 7I, 7O).

Discussion

This study reports a brief characterization of hAFSCs as a potential therapy in stroke animal models. Amniotic fluid was investigated as a new cell source for mesenchymal stem cells (MSCs) in the development of future cell-based transplantation. Thus, studies have suggested that AFSCs are possible mesenchymal precursors[32–34]. These cells possess a protein expression profile that is similar to mesenchymal cells, such as the expression of CD29, CD44, CD73, CD90, CD105, and CD166; and negative and/or low expression of CD14, CD31, CD34, CD45, CD106, CD133, and HLA-DR (Fig. 3A). However, their immune properties are still being assessed, although these cells have been regarded as possessing low immunogenicity. In addition, the hAFSCs also expressed homing markers and transcription factors, suggesting that this population may present important therapeutic characteristics such as plasticity, reduced immunogenicity, anti-inflammatory potential, and the ability to migrate to a site of tissue injury and inflammation, as well as playing a crucial role in the maintenance of pluripotency and self-renewal (Fig. 3B). Other recent studies have shown the immunomodulatory properties of these cells, which can inhibit the proliferation of T lymphocytes[33,34], and recent in vitro analysis has found that AFSCs modulate lymphocyte proliferation in different manners according to gestational age (i.e., those derived from first-trimester significantly

inhibited T-cell and natural killer cell proliferation, while second and third trimester were less efficient, and only inflammatory-primed second-trimester AFSCs could suppress B-cell proliferation)[33,35]. Our findings suggest that hAFSCs have an immune tolerance and/or immunosuppression effect, similar to that reported for other stem cells, and low risk of tumorigenicity.

The expression of specific pluripotency markers and genes in cells harvested from the amniotic fluid characterizes these cells as stem cells[33]. Here, we showed that these cells express OCT3/4, SOX2, Nanog, TRA1-60, and SSEA-4, by which it is suggested that they represent an intermediate stage between pluripotent embryonic stem cells (ESCs)[36–38] and lineage-restricted adult stem cells[39,40]. The expression of Tra-1-60 and SSEA-4 is associated with a "stemness" state, which suggests some overlap in specialized metabolic pathways between hESCs and pluripotent cells[40–42]. These findings suggest that these cells exhibit a wide range of differentiation potential, higher than the known potential of MSCs[43,44], and also support the idea that these cells may be biologically closer to hESCs that the counterpart adult MSCs. Moreover, the hAFSCs also expressed equivalently the markers CXCR4 and CCR2 (Fig. 3B), which are receptors for chemokines and have a variety of physiological functions, including immune system regulation, development and cell growth, cellular migration (cellular homing), and inflammatory regulation[43,44].

Recent studies have shown that AFSCs also possess gene expression profiles that are largely characteristic of undifferentiated cells[33,34]. In a related study by Antonucci

et al.[34], RT-PCR analysis showed that AFSCs express genes for Rex-1, SCF, GATA-4, vimentin, CK18, HLA-ABC, and FGF-5 throughout the culture period, and they express genes for BMP-4, nestin, AFP, and HNF-4α. As these genes regulate a host of different cell types, these observations suggest the AFSCs are able to differentiate into adipocytes, osteoblasts, chondrocytes, and neuronal cells; they can express many pluripotent stem cell-specific genes; and they proliferate well during ex vivo expansion[33,34]. Here, we also demonstrated that MION-Rh-labeled hAFSCs differentiated into adipocyte- and osteoblast-like cells, showing no cytotoxicity on labeling (Fig. 2B); our group standardized this labeling with published data[16].

Experimental focal cerebral ischemia of short duration followed by reperfusion, in this study, mimics the clinical syndrome of cerebral stroke. Cerebral ischemia is further documented as impairing sensorimotor ability[45], and it has been shown to exhibit marked deleterious effects on the somatosensory cortex and thus to cause resultant functional deficit[46]. Tests have been employed to assess the functional outcome of the sensorimotor center activity in the brain. Besides an elaborate ischemic insult produced in the focal cerebral region, ischemia has been shown to cause widespread neuronal tissue damage in the central nervous system, with consequent impairment of motor coordination and multiple sensory reflexes[47,48]. Thus, a set of modified neurological severity scores has been used to assess motor and exploratory capacity[49].

This study reports the therapeutic potential of hAFSC transplantation in an animal model of stroke via the caudal vein (intravenous). The labeled cells migrated to the ischemic focus (Fig. 5E.b), characterized by decreased infarct volume (Fig. 4) and improvement of motor deficit; this means that the attenuation of stroke induced behavioral changes (Fig. 6), possibly due to an increase in endogenous repair mechanisms, such as neurogenesis, angiogenesis, and immunomodulation.

It is well established that the ischemic lesion resulting from MCAo, which is the ischemic core, involves dopaminergic dysfunction in the frontal cortex and the striatum, mainly in the caudate nucleus and putamen[50], resulting in cognitive and motor changes[51], and in the anterior dorsal cortex, responsible for symmetry and stability of the forelegs and hind legs[52].

We showed that the intravenous transplantation of hAFSCs, 6 h after reperfusion, improved motor damage and exploratory behavior followed by reduction in infarct volume, demonstrated in the MRI images (Fig. 5C), within the first 24 h after hAFSC transplantation, progressively improving within 28 days (Fig. 6). These functional improvements in hAFSC-transplanted stroke animals coincided with increased cell proliferation in the penumbra area, suggesting the role of graft-induced host tissue repair in this brain remodeling process following stroke (Fig. 7D, 7J, and 7P).

The same behavior was not observed in animals receiving cell therapy 1 h and 24 h after reperfusion, in the first 24 h,

which showed less improvement than animals treated 6 h after reperfusion (Fig. 6). It is possible that the late onset of therapy, 24 h after reperfusion, may have extended the ischemic nucleus to the penumbra area, increasing the ischemic region and making the action of the trophic factors related to the immunosuppressive activity of these cells more difficult in the first 24 h, thus suggesting that an impediment in the corporate penumbra area to the ischemic core generates a better paracrine effect of these cells in this area, in the initial hours after the event. After 14 and 28 days of cell infusion, for treated animals both 1 and 24 h after the event, there was a more significant improvement over the first 24 h. AFSCs have been shown to express and secrete a number of factors that could potentially support neuroprotective and/or reparative functions, such as vascular endothelial growth factor, stromal cell-derived factor-1 (CXCL12), and IL-8, all of which regulate angiogenesis[17,53,54]. In fact, the pro-angiogenic capacity of these cells has been shown in mouse hind limb ischemia[17,54] and ischemic skin flap[17,55] models. Thus, the secretion of proangiogenic factors by these cells might contribute to improving functions in models of nervous system injury.

Other studies have suggested that transplanted adult stem cells may enhance the survival of host neurons through the release of trophic factors, stimulate endogenous repair through the recruitment of progenitor cells and promotion of neurite outgrowth, and render the peri-lesion environment less toxic and more advantageous to regeneration by modulating the immune response and scar formation[17,56]. These cells promote re-epithelialization, modulate differentiation and angiogenesis, and decrease inflammation, apoptosis, and fibrosis[57–60].

Transplanted hAFSCs may contribute to nervous system repair in two different ways. Exogenous cells may serve as direct replacements for lost or damaged cells; this requires that the cells differentiate into the appropriate neuronal subtypes, acquire functional properties of the desired cell types, and integrate into the existing circuitry. Another possibility is that transplanted cells may provide support for surviving host cells in the penumbra area, offer protection from the toxic environment surrounding the injury, and/or stimulate endogenous repair mechanisms[17,61–63], and we believe that our cells (hAFSCs) support functions in nervous system injury.

Preclinical data of the safety and efficacy of AFSCs suggest that individuals who suffer a stroke and show significant inflammation of the brain, or who display short-term memory loss due to the accompanying injury to the hippocampus, may be ideal candidates for future clinical trials of AFSC transplantation[1,33].

The lack of ethical barriers associated with the harvest of the hAFSCs, easy isolation and amplification of these cells, their ability to differentiate into other cell lines, and capacity to exert immunomodulatory effects make them an ideal cell source. Indeed, hAFSCs appear to have great potential for future clinical application in regenerative medicine,

especially for stroke therapy, since they seem to promote restorative mechanisms, such as neurogenesis, angiogenesis, and immunomodulation, and to contribute to functional improvement. Additional research needs to be done to determine the full therapeutic range of hAFSCs, and to identify the optimal time and best administration path for transplantation in clinically relevant stroke models. Discovering the true potential of these cells could lead to great advances in the fields of tissue engineering and regenerative medicine, and finally to the clinical application of these cells in stroke patients.

Ethical Approval

All animal experiments were conducted in accordance with the guidelines for animal experimentation determined by the UNIFESP Care Committee, and approved by the Committee on the Ethics of Animal Experiments of UNIFESP.

Statement of Human and Animal Rights

All animal experiments were conducted in accordance with the guidelines for animal experimentation determined by the UNIFESP Care Committee, and approved by the Committee on the Ethics of Animal Experiments of UNIFESP. In addition, ethical conditions were maintained, assuming all international rules of animal care outlined by the International Animal Welfare Recommendations and in accordance with local institutional animal welfare guidelines.

Statement of Informed Consent

Informed consent was obtained from all participants included in this study.

Declaration of Conflicting Interests

The authors declared no potential conflicts of interest with respect to the research, authorship, and/or publication of this article.

ORCID iD

Marcos Devanir Silva da Costa 🔘 https://orcid.org/0000-0003-3 552-6347

References

1. Tajiri N, Acosta S, Portillo-Gonzales GS, Aguirre D, Reyes S, Lozano D, Pabon M, Dela Peña I, Ji X, Yasuhara T, Date I, et al. Therapeutic outcomes of transplantation of amniotic fluid-derived stem cells in experimental ischemic stroke. Front Cell Neurosci. 2014;8:227.

2. Roger VL, Go AS, Lloyd-Jones DM, Benjamin EJ, Berry JD, Borden WB, Bravata DM, Dai S, Ford ES, Fox CS, Fullerton HJ, et al; American Heart Association Statistics Committee and Stroke Statistics Subcommittee. Executive summary: heart disease and stroke statistics—2012 update: a report from the American Heart Association. Circulation. 2012;125(1): 188–197.

3. Tajiri N, Acosta S, Glover LE, Bickford PC, Jacotte Simancas A, Yasuhara T, Date I, Solomita MA, Antonucci I, Stuppia L, Kaneko Y, et al. Intravenous grafts of amniotic fluid-derived stem cells induce endogenous cell proliferation and attenuate behavioral deficits in ischemic stroke rats. PloS One. 2012; 7(8):e43779.

4. Graham GD. Tissue plasminogen activator for acute ischemic stroke in clinical practice: a meta-analysis of safety data. Stroke. 2003;34(12):2847–2850.

5. Yip TR, Demaerschalk BM. Estimated cost savings of increased use of intravenous tissue plasminogen activator for acute ischemic stroke in Canada. Stroke. 2007;38(6): 1952–1955.

6. Antonucci I, Stuppia L, Kaneko Y, Yu S, Tajiri N, Bae EC, Chheda SH, Weinbren NL, Borlongan CV. Amniotic fluid as a rich source of mesenchymal stromal cells for transplantation therapy. Cell Transplant. 2011;20(6):789–795.

7. Kaneko Y, Hayashi T, Yu S, Tajiri N, Bae EC, Solomita MA, Chheda SH, Weinbrein NL, Parolini O, Borlongan CV. Human amniotic epithelial cells express melatonin receptor MT1, but not melatonin receptor MT2: a new perspective to neuroprotection. J Pineal Res. 2011;50(3):272–280.

8. Manuelpillai U, Moodley Y, Borlongan CV, Parolini O. Amniotic membrane and amniotic cells: potential therapeutic tools to combat tissue inflammation and fibrosis? Placenta. 2011;32(Suppl 4):S320–S325.

9. Yu SJ, Soncini M, Kaneko Y, Hess DC, Parolini O, Borlongan CV. Amnio: a potent graft source for cell therapy in stroke. Cell Transplant. 2009;18(2):111–118.

10. Borlongan CV, Koutouzis TK, Jorden JR, Martinez R, Rodriguez AL, Poulos SG, Freeman TB, McKeown P, Cahil DW, Nishino H, Sanberg PR. Neural transplantation as an experimental treatment modality for cerebral ischemia. Neurosci Biobehav Rev. 1999;21(1):79–90.

11. Nishino H, Borlongan CV. Restoration of function by neural transplantation in the ischemic brain. Prog Brain Res. 2000; 127:461–476.

12. Eriksson PS, Perfilieva E, Bjork-Eriksson T, Alborn AM, Nordborg C, Peterson DA, Gage FH. Neurogenesis in the adult human hippocampus. Nat Med. 1998;4(11):1313–1317.

13. Curtis MA, Kam M, Nannmark U, Anderson MF, Axell MZ, Wikkelso C, Holtas S, van Roon-Mom WM, Bjork-Eriksson T, Nordborg C, Frisén J, et al. Human neuroblasts migrate to the olfactory bulb via a lateral ventricular extension. Science. 2007;315(5816):1243–1249.

14. Banerjee S, Williamson DA, Habib N, Chataway J. The potential benefit of stem cell therapy stroke: an update. Vasc Health Risk Manag. 2012;8:569–580.

15. Jin K, Wang X, Xie L, Mao XO, Zhu W, Wang Y, Shen J, Mao Y, Banwait S, Greenberg DA. Evidence for stroke-induced neurogenesis in the human brain. Proc Natl Acad Sci USA. 2006;103(35):13198–13202.

16. Sibov TT, Pavon LF, Miyaki LA, Mamani JB, Nucci LP, Alvarim LP, Silveira PH, Marti LC, Gamarra LF. Umbilical cord mesenchymal stem cells labeled with multimodal iron oxide nanoparticles with fluorescent and magnetic properties: application for in vivo cell tracking. Int J Nanomedicine. 2014; 9:337–350.

17. Rennie K, Haukenfrers J, Ribecco-Lutkiewicz M, Ly D, Jezierski A, Smith B, Zurakowski B, Martina M, Gruslin A, Bani-Yaghoub M. Therapeutic potential of amniotic fluid-derived cells for treating the injured nervous system. Biochem Cell Biol. 2013;91(5):271–286.

18. Arnhold S, Gluer S, Hartmann K, Raabe O, Addicks K, Wenisch S, Hoopmann M. Amniotic-fluid stem cells: growth dynamics and differentiation potential after a CD117 based selection procedure. Stem Cells Int. 2011;2011:715341.

19. Aronoff R, Matyas F, Mateo C, Ciron C, Schneider B, Petersen CC. Long-range connectivity of mouse primary somatosensory barrel cortex. Eur J Neurosci. 2010;31(12):2221–2233.

20. Arvidsson A, Collin T, Kirik D, Kokaia Z, Lindvall O. Neuronal replacement from endogenous precursors in the adult brain after stroke. Nat Med. 2002;8(9):963–970.

21. Prusa AR, Hengstschlager M. Amniotic fluid cells and human stem cell research: a new connection. Med Sci Monit. 2002; 8(11):RA253–RA257.

22. Fauza D. Amniotic fluid and placental stem cell. Best Pract Res Clin Obstet Gynaecol. 2004;18(6):877–891.

23. Kim BS, Chun SY, Lee JK, Lim HJ, Bae JS, Chung HY, Atala A, Soker S, Yoo JJ, Know TG. Human amniotic fluid stem cell injection therapy for urethral sphincter regeneration in an animal model. BMC Med. 2012;10:94.

24. De Coppi P, Bartsch G Jr, Siddiqui MM, Xu T, Santos CC, Perin L, Mostoslavsky G, Serre AC, Snyder EY, Yoo JJ, Furth ME, et al. Isolation of amniotic stem cells lines with potential for therapy. Nat Biotechnol. 2007;25(1):100–106.

25. In t Anker PS, Scherjon SA, Kleijburg-van der Keur C, Noort WA, Claas FH, Willemze R, Fibbe WE, Kanhai HH. Amniotc fluid as a novel source of mesenchymal stem cells for therapeutic transplantation. Blood. 2003;102(4):1548–1549.

26. Koizumi J, Nakazawa T, Yoshida Y. Reperfusable brain infarction model in the rat. Proceedings of the 10th Meeting of the Japanese Stroke Society; 1985; Kyota, Japan; p 159.

27. Longa EZ, Weinstein PR, Carlson S, Cummins R. Reversible middle cerebral artery occlusion without craniectomy in rats. Stroke. 1989;20(1):84–91.

28. Anderson BJ, Alcantara AA, Geenough WT. Changes in synaptic organization of the rat cerebellar cortex. Neurobiol Learn Mem. 1996;66(2):221–229.

29. Chu CJ, Jones TA. Experience-dependent structural plasticity in cortex heterotopic to focal sensorimotor cortical damage. Exp Neurol. 2000;166(2):403–414.

30. Hurtado O, De Cristóbal J, Sánchez V, Lizasoain I, Cárdenas A, Pereira MP, Colado MI, Leza JC, Lorenzo P, Moro MA.

Inhibition of glutamate release by delaying ATP fall accounts for neuroprotective effects of antioxidants in experimental stroke. FASEB J. 2003;17(14):2082–2084.

31. Garcia JH, Wagner S, Liu KF, Hu XJ. Neurological deficit and extent of neuronal necrosis attributable to middle cerebral artery occlusion in rats: statistical validation. Stroke. 1995; 26(4):627–634.

32. Wang D, Chen R, Zhong X, Fan Y, Lai W, Sun X. Levels of cd105 cells increase and cell proliferation decreases during s-phase arrest of amniotic fluid cells in long-term culture. Exp Ther Med. 2014;8(5):1604–1610.

33. Elias M, Hoover J, Nguyen H, Reyes S, Lawton C, Borlongan CV. Stroke therapy: the potential of amniotic fluid-derived stem cells. Future Neurol. 2015;10(4):321–326.

34. Antonucci I, Pantalone A, Tete S, Salini V, Borlongan CV, Hess D, Stuppia L. Amniotic fluid stem cells: a promising therapeutic resource for cell-based regenerative therapy. Curr Pharm Des. 2012;18(13):1846–1863.

35. Di Trapani M, Bassi G, Fontana E, Giacomello L, Pozzobon M, Guillot PV, De Coppi P, Krampera M. Immune regulatory properties of cd117(pos) amniotic fluid stem cells vary according to gestational age. Stem Cells Dev. 2015;24(1):132–143.

36. Evans MJ, Kaufman MH. Establishment in culture of pluripotential cells from mouse embryos. Nature. 1981;292(5819): 154–156.

37. Martin GR. Isolation of a pluripotent cell line from early mouse embryos cultured in medium conditioned by teratocarcinoma stem cells. Proc Natl Acad Sci USA. 1981;78(12):7634–7638.

38. Thomson JA, Itskovitz-Eldor J, Shapiro SS, Waknitz MA, Swiergiel JJ, Marshall VS, Jones JM. Embryonic stem cell lines derived from human blastocysts. Science. 1998; 282(5391):1145–1147.

39. De Coppi P, Bartsch G Jr, Siddiqui MM, Xu T, Santos CC, Perin L, Mostoslavsky G, Serre AC, Snyder EY, Yoo JJ, Furth ME, et al. Isolation of amniotic stem cell lines with potential for therapy. Nat Biotechnol. 2007;25(1):100–106.

40. Pozzobon M, Piccoli M, De Coppi P. Stem cells from fetal membranes and amniotic fluid: markers for cell isolation and therapy. Cell Tissue Bank. 2014;15(2):199–211.

41. Llancheran S, Michalska A, Peh G, Wallace EM, Pera M, Manuelpillai U. Stem cells derived from human fetal membranes display multilineage differentiation potential. Biol Reprod. 2007;77(3):577–588.

42. Miki T, Lehmann T, Cai H, Stolz DB, Strom SC. Stem cell characteristics of amniotic epithelial cells. Stem Cells. 2005; 23(10):1549–1559.

43. Ji JF, He BP, Dheen S, Tay SS. Expression of chemokine receptors CXCR4, CCR2, CCR5 and CX3CR1 in neural progenitor cells isolated from the subventricular zone of the adult rat brain. Neurosci Lett. 2004;355(3):236–240.

44. Rollins BJ. Chemokines. Blood. 1997;90(3):909–928.

45. Dobkin BH. The rehabilitation of elderly stroke patients. Clin Geriat Med. 1991;7(3):507–523.

46. Zhang L, Chen J, Li Y, Zhang ZG, Chopp M. Quantitative measurement of motor and somatosensory impairments mild

(30 min) and severe (2 h) transient middle cerebral artery occlusion in rats. J Neurol Sci. 2000;174(2):141–146.

47. Johansson BB. Functional outcome in rats transferred to an enriched environment 15 days after focal brain ischemia. Stroke. 1996;27(2):324–326.

48. Rogers DC, Campbell CA, Stretton JL, Mackay KB. Correlation between motor impairment and infarct volume after permanent and transient middle cerebral artery occlusion in rat. Stroke. 1997;28(10):2060–2066.

49. Pietá DC, Martins LMN, Presti-Torres J, Dornelles A, Garcia VA, Siciliani SF, Rewsaat GM, Constantino L, Budni P, Dal-Pizzol F, Schroder N. Memantine reduces oxidative damage and enhances long-term recognition memory in aged rats. Neuroscience. 2007;146(4):1719–1725.

50. Devries AC, Nelson RJ, Traystman RJ, Hurn PD. Cognitive and behavioral assessment in experimental stroke research: will it prove useful? Neurosci Biobehav Rev. 2001;25(4): 325–342.

51. Pandolfo P, Machado NJ, Kofalvi A, Takahashi RN, Cunha RA. Caffeine regulates frontocorticostriatal dopamine transporter density and improves attention and cognitive deficits in an animal model of attention deficit hyperactivity disorder. Eur Neuropsychopharmacol. 2013;23(4):317–328.

52. Wahl F, Allix M, Plotkine M, Boulu RG. Neurological and behavioral outcomes of focal cerebral ischemia in rats. Stroke. 1992;23(2):267–272.

53. Yoon BS, Moon JH, Jun EK, Kim J, Maeng I, Kim JS, Lee JH, Baik CS, Kim A, Cho S, Lee JH, et al. Secretory profiles and wound healing effects of human amniotic fluid-derived mesenchymal stem cells. Stem Cells Dev. 2010;19(6): 887–902.

54. Mirabella T, Cilli M, Carlone S, Cancedda R, Gentili C. Amniotic liquid derived stem cells as reservoir of secreted angiogenic factors capable of stimulating neo-arteriogenesis in an ischemic model. Biomaterials. 2011;32(15):3689–3699.

55. Mirabella T, Hartinger J, Lorandi C, Gentili C, van Griensven M, Cancedda R. Proangiogenic soluble factors from amniotic fluid stem cells mediate the recruitment of endothelial progenitors in a model of ischemic fasciocutaneous flap. Stem Cells Dev. 2012;21(12):2179–2188.

56. Chiu AY, Rao MS. Cell-based therapy for neural disorders-anticipating challenges. Neurotherapeutics. 2011;8(4): 744–752.

57. Parolini O, Soncini M, Evangelista M, Schmidt D. Amniotic membrane and amniotic fluid-derived cells: potential tools for regenerative medicine? Regen Med. 2009;4(2);275–291.

58. Parolini O, Alviano F, Betz AG, Bianchi DW, Götherström C, Manuelpillai U, Mellor AL, Ofir R, Ponsaerts P, Scherjon SA, Weiss ML, et al. Meeting report of the first conference of the International Placenta Stem Cell Society (IPLASS). Placenta. 2011;32(suppl 4):S285–S290.

59. Uchida S, Inanaga Y, Kobayashi M, Hurukawa S, Araie M, Sakuragawa N. Neurotrophic function of conditioned medium from human amniotic epithelial cells. J Neurosci Res. 2000; 62(4):585–590.

60. Liu T, Wu J, Huang Q, Hou Y, Jiang Z, Zang S, Guo L. Human amniotic epithelial cells ameliorate behavioral dysfunction and reduce infarct size in the rat middle cerebral artery occlusion model. Shock. 2008;29(5):603–611.

61. Boucherie C, Hermans E. Adult stem cell therapies for neurological disorders: benefits beyond neuronal replacement? J Neurosci Res. 2009;87(7):1509–1521.

62. De Feo D, Merlini A, Laterza C, Martino G. Neural stem cell transplantation in central nervous system disorders: from cell replacement to neuroprotection. Curr Opin Neurol. 2012;25(3): 322–333.

63. Einstein O, Ben-Hur T. The changing face of neural stem cell therapy in neurologic diseases. Arch Neurol. 2008;65(4): 452–456.